Spin-gap state and superconducting correlations in a one-dimensional dimerized t-J model

Masatoshi Imada
Institute for Solid State Physics, University of Tokyo, Roppongi 7-22-1, Minato-ku, Tokyo 106, Japan
(Received 18 December 1991; revised manuscript received 8 June 1992)

The phase diagram of one-dimensional dimerized t-J model is investigated by exact-diagonalization, quantum tranfer-matrix, and quantum Monte Carlo methods. The spin gap persists near but away from half-filling as well as in a strongly dimerized region, while the charge can be described as a Tomonaga-Luttinger liquid in the entire region. The spin-gap region extends to the weak-dimerization region as well as to the Haldane-gap region. Critical exponents of various correlation functions are discussed. The pairing correlation shows remarkable enhancement and by far dominates over other correlations near half-filling. At quarter filling, charge-gap formation is observed.

I. INTRODUCTION

More than one decade ago, the phase diagram of the one-dimensional (1D) extended Hubbard model was obtained by consideration of both exact solutions of the model for some special parameters and the weak-coupling renormalization-group analysis known as g-ology.[1,2] The 1D extended Hubbard model describes a class of strongly correlated systems and is defined by the following Hamiltonian:

$$H=-t\sum_{\langle ij\rangle,\sigma}(c_{i\sigma}^{\dagger}c_{j\sigma}+\text{H.c.})+U\sum_{i}n_{i\uparrow}n_{i\downarrow}+V\sum_{\langle ij\rangle}n_{i}n_{j}\ . \tag{1.1}$$

In the continuum limit, it is related to the Fermi-gas model. The Fermi-gas model has two fixed points, namely the Tomonaga-Luttinger (TL) fixed point and the Luther-Emery (LE) fixed point. The TL fixed point governs the positive backward-scattering region ($g_1>0$) and the LE region is represented by $g_1<0$ to which the Luther-Emery exact solution[3] belongs. The essential difference between the TL and LE regions lies in the spin degrees of freedom. The TL region is characterized by the so-called TL liquid both for spin and charge degrees of freedom, while in the LE region, the charge is described by the TL liquid but the spin degrees of freedom have a gap. In terms of the extended Hubbard model away from half-filling, the TL region corresponds to $U>2V$.

Recently the critical exponent of the TL liquid in the TL region has been determined for the entire range of interaction strength in the Hubbard model with the help of the Bethe ansatz solution with an assumption based on conformal field theory.[4,5] The critical exponent of the supersymmetric t-J model has also been determined in a similar way.[6]

From these analyses, the previous speculation on the TL fixed point for the extended Hubbard model has been confirmed on a firmer basis. The extended Hubbard model with $U>2V$ and the t-J model, except at very low filling, show similar behavior with both gapless spin and charge degrees of freedom. In a region of the U-V or t-J diagram, triplet pairing is the most dominant correlation for the uniform part followed by logarithmically weaker singlet pairing correlation. This region is sandwiched by the spin-density-wave (SDW) dominating region and the phase-separation area. In the entire region of the TL fixed-point class, the spin is gapless and the spin susceptibility remains finite at temperature $T=0$.

Essentially different behavior is seen in the LE region, $U<2V$ where the attractive interaction plays a crucial role. The spin has a gap instead of the TL liquid. In the ground state, either the charge-density-wave (CDW) or the singlet pairing correlation is the most dominant correlation, depending on the parameter value. The attractive Hubbard model belongs to the LE region. The phase diagram of the extended Hubbard model away from half-filling is summarized in Fig. 1.

In contrast to the non-half-filled band, the charge may have a gap at half-filling. For example, the repulsive Hubbard model ($U>0, V=0$) has the charge gap $\Delta_c>0$ while the spin is gapless. The attractive Hubbard model has both the charge gap $\Delta_c>0$ and the spin gap $\Delta_s>0$ for $U<0<V$. Therefore we can realize all the possibilities, namely (1) $\Delta_c=0$, $\Delta_s=0$ (LE region), (2) $\Delta_c=0$, $\Delta_s>0$ (TL region), (3) $\Delta_c>0$, $\Delta_s=0$ (repulsive Hubbard at half-filling), and (4) $\Delta_c>0$, $\Delta_s>0$ (attractive Hubbard

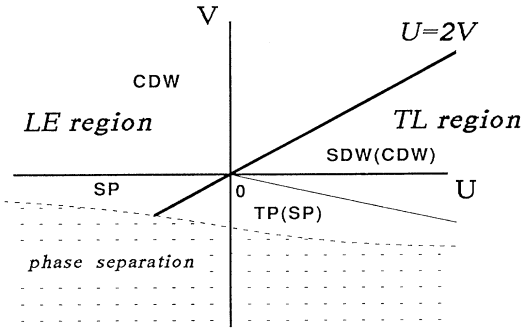

FIG. 1. Schematic phase diagram of the extended Hubbard model away from half-filling. SP, TP, CDW, and SDW indicate that the dominant correlations are singlet pairing, triplet pairing, CDW, and SDW, respectively. Parenthesized correlations show logarithmically faster decay than the dominant ones.

with $V>0$ at half-filling).

In 1D systems, correlation functions decay either exponentially or algebraically as a function of distance according to model parameter value and filling. We introduce four types of correlation functions: The CDW correlation

$$C_{\mathrm{CDW}}(r_i-r_j)=\langle n_i n_j\rangle-\langle n_i\rangle\langle n_j\rangle\ , \tag{1.2a}$$

the SDW correlation

$$C_{\mathrm{SDW}}(r_i-r_j)=\langle \mathbf{S}_i\cdot\mathbf{S}_j\rangle\ , \tag{1.2b}$$

the singlet pairing correlation

$$C_{\mathrm{SP}}(r_i-r_j)=\langle O_{Si}^{\dagger}O_{Sj}\rangle\ , \tag{1.2c}$$

and the triplet pairing correlation

$$C_{\mathrm{TP}}(r_i-r_j)=\langle O_{Ti}^{\dagger}O_{Tj}\rangle\ , \tag{1.2d}$$

where

$$O_{Si}=\frac{1}{\sqrt{2}}(c_{i\uparrow}c_{i+1\downarrow}-c_{i\downarrow}c_{i+1\uparrow}) \tag{1.3a}$$

and

$$O_{Ti}=\frac{1}{\sqrt{2}}(c_{i\uparrow}c_{i+1\downarrow}+c_{i\downarrow}c_{i+1\uparrow})\ . \tag{1.3b}$$

In the TL region, the asymptotic forms of these correlations are given by

$$C_{\mathrm{CDW}}(r)\sim\frac{a_0}{r^2}+a_1\cos(2k_F r)r^{-(\theta_c+1)}\ , \tag{1.4a}$$

$$C_{\mathrm{SDW}}(r)\sim\frac{b_0}{r^2}+b_1\cos(2k_F r)r^{-(\theta_c+1)}\ , \tag{1.4b}$$

$$C_{\mathrm{SP}}(r)\sim c_1 r^{-(1/\theta_c+1)}+c_2\cos(2k_F r)r^{-(\theta_c+1/\theta_c)}\ , \tag{1.4c}$$

$$C_{\mathrm{TP}}(r)\sim d_1 r^{-(1/\theta_c+1)}\ , \tag{1.4d}$$

where the critical exponents of the algebraic decays are characterized by a single parameter θ_c. We have dropped the logarithmic corrections in these expressions. Although C_{CDW} and C_{SDW} have the same critical exponent for the oscillating part, the logarithmic correction is $\ln^{-3/2}(r)$ for C_{CDW} and $\ln^{1/2}(r)$ for C_{SDW}, and hence C_{SDW} shows logarithmically larger correlation.[7,8] The same is true for the uniform part of C_{SP} and C_{TP}, where C_{TP} has logarithmically larger correlation than C_{SP}.

In the LE region, the spin has a gap and C_{SDW} and C_{TP} decays exponentially. Because the contribution from spin excitations vanishes, the critical exponents of C_{CDW} and C_{SP} also change and the asymptotic forms are given by

$$C_{\mathrm{CDW}}(r)\sim\frac{a_0'}{r^2}+a_1'\cos(2k_F r)r^{-\theta_c}\ , \tag{1.5a}$$

$$C_{\mathrm{SP}}(r)\sim c_1' r^{-1/\theta_c}\ . \tag{1.5b}$$

Therefore, the singlet pairing correlation becomes dominant over the CDW correlation if $\theta_c>1$. The temperature dependence of the CDW and the pairing susceptibilities should be

$$\chi_{\mathrm{CDW}}\sim T^{-2+\theta_c}\ , \tag{1.6a}$$

and

$$\chi_{\mathrm{SP}}\sim T^{-2+(1/\theta_c)}\ , \tag{1.6b}$$

respectively, at low temperatures.

In connection with mechanisms of singlet superconductivity, it is obvious that the spin degrees of freedom have to die out in the singlet superconducting state irrespective of its symmetry and dimensionality. Below the s-wave critical temperature, the spin susceptibility falls exponentially and it is replaced with a power law in the d-wave state. In any case the spin susceptibility is, of course, zero at $T=0$. These features should be seen, for example, in the attractive Hubbard model. These are a general aspect of singlet superconducting state.

In one dimension, although the superconducting long-range order is absent, all the 1D models corresponding to superconducting multidimensional systems such as the attractive Hubbard model show vanishing spin susceptibility at $T=0$. This is related to the fact that the spin gap appears even from the short-range part of particle-particle correlation and it is not sensitive to the dimensionality, while superconducting long-range order itself is realized only in a part of this region. In this respect, although we have to be careful about the difference between the 1D system and its multidimensional analogy, it is important to extract a model belonging to the LE region from essentially repulsive systems even in 1D.

The author has proposed[9,10] a mechanism of superconductivity where the dimerization of spins from either extrinsic or intrinsic origin triggers a spin-gap formation and it is directly connected with the superconductivity.

In 1D systems,[9,10] the author has examined several possibilities such as the dimerized t-J model, a frustrated t-J model with the next-nearest-neighbor exchange and the spin-1 model with the Haldane-gap state. In this paper, the dimerized t-J model is investigated in detail and the quantitative analysis of critical exponents is given. This model is also related to the spin-1 system with the Haldane gap as we will discuss below. The region of Luther-Emery fixed point is investigated and its pairing correlation is shown with the help of the exact diagonalization of small clusters and the numerical transfer-matrix method. A possible importance of the dimer pairing mechanism in real high-T_c cuprates has been discussed in a separate paper[11] by a mean-field analysis of the superconducting phase, where several novel features of this pairing have appeared and they have been compared with experimental indications. In Sec. II, we introduce the dimerized t-J model. The results from the exact diagonalization and the numerical transfer matrix are presented in Sec. III. Section IV is devoted to conclusions and discussions.

II. DIMERIZED t-J MODEL

The one-dimensional dimerized t-J model Hamiltonian is defined by

$$H=H_t+H_J\ , \tag{2.1a}$$

$$H_t=-t\sum_{\langle ij\rangle\sigma}P_d(c^\dagger_{i\sigma}c_{j\sigma}+c^\dagger_{j\sigma}c_{i\sigma})P_d\ , \tag{2.1b}$$

$$H_J=J\sum_i[1+\gamma(-1)^i][\mathbf{S}_i\cdot\mathbf{S}_{i+1}-\tfrac{1}{4}n_in_{i+1}]\ , \tag{2.1c}$$

where, on the ith site of the 1D ring, the fermion creation (annihilation) operator $c^\dagger_{i\sigma}(c_{i\sigma})$, the spin-$\frac{1}{2}$ operator $\mathbf{S}_i$ and the number operator n_i are introduced. We assume $0\le\gamma\le1$. The projection operator P_d is introduced to prohibit the double occupation of fermions on the same site. This model will be sometimes discussed in a modified form where $\mathbf{S}_i\cdot\mathbf{S}_{i+1}-\frac{1}{4}n_in_{i+1}$ in H_J is replaced with $\mathbf{S}_i\cdot\mathbf{S}_{i+1}$. Namely, the modified form of the Hamiltonian is defined as

$$H'=H_t+H'_J\ , \tag{2.2a}$$

$$H'_J=J\sum_i[1+\gamma(-1)^i]\mathbf{S}_i\cdot\mathbf{S}_{i+1}\ . \tag{2.2b}$$

Qualitatively, correlation functions of (2.2) show similar behavior to (2.1). In the half-filled case, the Hamiltonians (2.1) and (2.2) are reduced to a dimerized Heisenberg model expressed only by H'_J. This model H'_J has a spin gap for $\gamma\neq0$. Its quantitative features have been examined by many authors[12–14] with various methods ranging from the Hartree-Fock, bosonization, phase Hamiltonian to numerical studies. Two quantities characterize the dimerization of spins. The first quantity is the gain of the ground-state energy E_0 in the presence of the dimerization:

$$\Delta E\equiv E_0(\gamma)-E_0(\gamma=0)=-A\gamma^a\ . \tag{2.3}$$

The second is the energy gap between the first excited-state energy E_1 and the ground-state energy E_0:

$$E_{\rm gap}=E_1(\gamma)-E_0(\gamma)=B\gamma^b\ . \tag{2.4}$$

The critical exponents a and b are defined for small γ. Although the Hartree-Fock approximation predicts $a=2$ except the logarithmic correction, the numerical diagonalization study with a finite-size scaling analysis shows much smaller value $a\sim1.4$. Because the lattice distortion loses the elastic energy proportional to γ^2, the numerical results show that the lattice is unstable to the spin-Peierls distortion. Then the energy gap opens in the spin excitation spectrum as in (2.4), where the critical exponent is estimated to be $b\sim0.8$ in the diagonalization of finite-size systems combined with the finite-size scaling study,[12] while bosonization and the phase Hamiltonian approach predict a little bit smaller values.

It should also be noted that, in (2.1) and (2.2), one of the exchange interactions expressed by $J(1-\gamma)$ becomes ferromagnetic for $\gamma>1$. The dimerized t-J model at half-filling is mapped to the spin-1 Heisenberg model if two kinds of exchange bonds J_1 and J_2 are taken such that J_1 is an antiferromagnetic (positive) constant with ferromagnetic J_2 in the limit $J_2\to-\infty$ as pointed out by Hida.[15] In fact, it has been shown that the spin gap in the dimerized Heisenberg model and the Haldane gap in the spin-1 system are continuously connected with each other in the parameter space of the dimerization at half-filling.[15] Therefore, the spin gap exists for $0<\gamma\le\infty$, at least at half-filling. Because $J_2=J(1-\gamma)$ changes the sign to ferromagnetic by increasing γ through 1, we are able to see the crossover between the weak-dimerization and the Haldane-gap region in (2.1) and (2.2) not only at half-filling but also away from half-filling where the effect of doping can be seen. We will also note that the doping of Haldane-gap system with spin-half mobile fermions may lead to interesting and rich physics as we will discuss below.

When the system is adopted away from half-filling, the charge degrees of freedom may participate in low-energy excitations. We first consider the case of strongly dimerized limit $J\gg t$ and $1-\gamma\ll1$ to elucidate the meaning of the spin-gap formation in the non-half-filled case. In this limit, the ground state of the half-filled system is described by independent singlet paris, where pairs are formed on the stronger bonds. When even number of holes are doped, in the lowest order perturbation of t/J, a hole always makes a pair with another hole on the stronger dimerized bonds to gain the singlet formation energy $3(1+\gamma)J/4$. Hopping of the holes only occurs as a pair tunneling through the virtual pair breaking in the fourth order of t/J. The Hilbert space of the effective Hamiltonian may be expanded only by the singlet Bose operator

$$\mathcal{S}^\dagger_i=\frac{1}{\sqrt{2}}(c^\dagger_{i\uparrow}c^\dagger_{i+1\downarrow}-c^\dagger_{i\downarrow}c^\dagger_{i+1\uparrow}) \tag{2.5}$$

for even site i. The effective Hamiltonian has the form

$$H_{\rm eff}=-\tilde{t}(\mathcal{S}^\dagger_i\mathcal{S}_{i+2}+\text{H.c.})\ , \tag{2.6}$$

where

$$\tilde{t}=\left[\frac{4}{3}\right]^3\frac{t^4}{\{J(1+\gamma)\}^2}\left\{\frac{1}{J(1+\gamma)}+\frac{1}{2J\gamma}\right\}\ . \tag{2.7}$$

The Hamiltonian (2.6) is the same as the effective Hamiltonian of the attractive Hubbard model in the strong-coupling limit. In the strong-coupling limit of the attractive Hubbard model, the pair hopping $\tilde{t}$ is given by

$$\tilde{t}=2\bar{t}^2/|U|\ ,$$

where U is the on-site attractive interaction and $\bar{t}$ is the fermion transfer energy. Two paired sites on a stronger bond in the dimerized t-J model correspond to one site in the attractive Hubbard model. A remarkable point in the dimerized t-J model is that it does not show phase separation in the strongly dimerized limit in contrast with the case of large J/t in the uniform t-J model.

The 1D attractive Hubbard model belongs to the Luther-Emery (LE) region except in the half-filled case. In the half-filled case both the spin and charge have gaps and the long-range CDW order appears in the ground state for $U<0$ and $V>0$. Corresponding to this fact, the dimerized t-J model has a charge gap in the quarter-filled case at least in the strongly dimerized limit and the long-range CDW order exists. Except for quarter filling, the charge gap closes and the charge degrees of freedom belong to the TL liquid, while the spin has a gap at least in

the strongly dimerized limit.

Therefore, it is clarified that the spin gap seen in the half-filled band persists away from half-filing at least in the strongly dimerized limit. As in the case of the attractive Hubbard model, the singlet pairing correlation is dominant in this LE region. For smaller values of J/t, the numerical analysis is the only available tool to see quantitative features of the spin gap and the pairing correlation, which will be discussed in the next section.

III. NUMERICAL RESULTS

In this section, results obtained from the exact diagonalization of finite clusters are presented to discuss the region of intermediate strength of J/t. The exact diagonalization has been performed up to 16 sites using the standard Lanczos algorithm. We also discuss finite temperature properties computed by the numerical transfer-matrix method for large system size. The algorithm of the numerical transfer-matrix method is described in Ref. 16. We will mainly show results obtained from the Hamiltonian (2.1) and they will be given except the cases where (2.2) is specified. Throughout this paper, the energy scale is set by $t=1$.

The chemical potential $\mu(\rho)$ at the filling ρ is defined by

$$\mu\left[\frac{2n+1}{N}\right]=\frac{1}{2}[E_0(n+1,n+1)-E_0(n,n)] . \quad (3.1)$$

Here $E_0(n,m)$ is the total ground-state energy of n up-spin and m down-spin fermions in the system of size N. When charge gap opens, it is defined as

$$\Delta_c\left[\frac{2n}{N}\right]=\mu\left[\frac{2n-1}{N}\right]-\mu\left[\frac{2n+1}{N}\right] . \quad (3.2)$$

If the charge gap vanishes in the thermodynamic limit, the charge compressibility $\kappa(\rho)$ is obtained from

$$\kappa\left[\frac{2n}{N}\right]=\frac{2}{N[\mu((2n+1)/N)-\mu((2n-1)/N)]} . \quad (3.3)$$

Since the ground state is a singlet at zero magnetic field, the spin gap is obtained from the energy difference between the lowest triplet energy and the single ground-state energy as

$$\Delta_s\left[\frac{2n}{N}\right]=E_0(n+1,n-1)-E_0(n,n) . \quad (3.4)$$

The spin and the charge gaps have been computed for finite clusters up to 16 sites by using the Lanczos method and they are extrapolated to the thermodynamic limit. To make the extrapolation more reliable, the quantum Monte Carlo results up to 32 sites have also been used. The method of the Monte Carlo calculation is based on the standard checkerboard algorithm, which is discussed in Sec. 2.7 of Ref. 17. The Monte Carlo calculation can be performed for larger lattices than the Lanczos method but with statistical errors and provides complementary results. The critical exponent θ_c is obtained from the charge compressibility κ and the charge velocity v_c with the help of the relationship[18,19]

$$\theta_c=\pi v_c\kappa/2 . \quad (3.5)$$

The charge velocity is calculated from

$$v_c=\frac{N}{2\pi}[E_1(n,n)-E_0(n,n)] , \quad (3.6)$$

where E_1-E_0 is the charge excitation energy. If the charge gap is absent, finite-size effects for v_c and κ are small. Therefore, in this paper, we will show exact diagonalization results on θ_c, v_c, and κ in the 16-site system, which is expected to be close to thermodynamic results.

Figure 2 illustrates the spin gap as a function of the dimerization γ and the filling. It shows that the gap opens at a finite dimerization γ_c for a fixed concentration of holes. The threshold value γ_c tends to vanish if the filling ρ approaches the half-filled. This suggests that the spin gap Δ_s is finite for any positive γ if the filling is sufficiently close to the half-filled. The TL region with spin-gapless ground state seen in the uniform t-J model may be adiabatically continuated with the spin-gapless region of Fig. 2 if the system sufficiently deviates from half-filling. On the other hand, at half-filling, the spin-gapless ground state is unstable against the arbitrarily small dimerization perturbation. The LE region with a spin gap extends to a weaker and weaker-dimerization region for the system nearer to half-filling, while the TL region shrinks. If $\gamma>1.0$, one of the two types of bonds is ferromagnetic and the crossover to the Haldane-gap region may be seen as discussed above. We notice that the spin-gap region seen in the weak dimerization region is continuously connected with the Haldane-gap region even in the non-half-filled case. It is generally seen that the gap persists more deeply away from the half-filled in the Haldane-gap region ($\gamma>1$) than in the weak-dimerization region.

Figure 3 shows overall sketch of the phase diagram for spin and charge gap at $t=1$ and $\gamma=1$. We note this parameter gives a typical intermediate point in the parameter space of spin-gap region as we have seen in Fig. 2. Because the behavior is qualitatively similar in the whole region of finite spin gap, we will mainly show the data at this parameter value to discuss the nature of the spin-gap

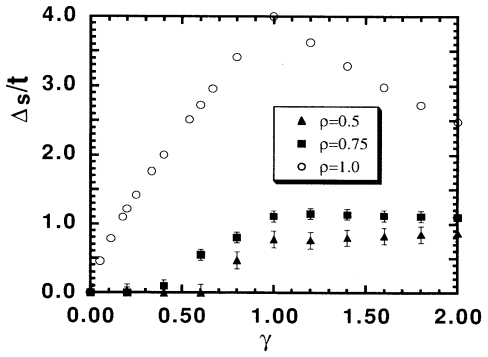

FIG. 2. Spin gap Δ_s/t as a function of the dimerization γ for the filling $\rho=0.5$, 0.75, and 1.0. For the part $\gamma\geq 1.0$, $(1+\gamma)J/2t$ is fixed at 1.0, while for $\gamma\leq 1.0$, J/t is fixed at 2.0.

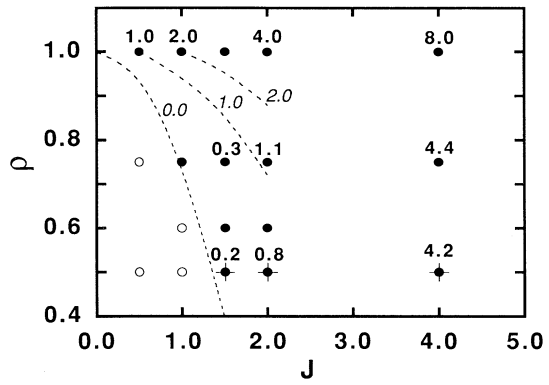

FIG. 3. Phase diagram of spin and charge gap in the plane of J and filling factor ρ for the case $\gamma=1$ and $t=1$. Filled circles show the existence of finite spin gap, while open circles show the absence. The values beside the filled circles show the spin gap Δ_s in the thermodynamic limit. The cross points indicate finite charge gap. The curves are for guide to the eyes to have qualitative idea about contour lines of the spin gap.

region. Although the half-filled case with $\gamma=1$ has a trivial solution with independent local singlets, it shows rich and highly nontrivial structure away from half-filling as we will see below. The spin gap present in the strongly dimerized limit persists into intermediate values of J/t and has larger value near half-filling. In particular, the spin gap seems to be present at smaller J/t when one approaches half-filling. This result seems to suggest that the spin gap does not close at arbitrarily small J/t if the filling is sufficiently close to half-filling. For smaller values of γ, the spin gap becomes small. However, the qualitative feature remains the same. Quantitative aspects and critical exponents in the limit of small dimerization away from half-filling remain for future study. The spin-gap formation is also observed in finite temperature results. Figure 4 illustrates the uniform spin susceptibility χ calculated by the numerical transfer-matrix method with the Hamiltonian (2.2).

In the strongly dimerized limit, the charge gap opens at quarter filling as discussed in Sec. II. This is actually

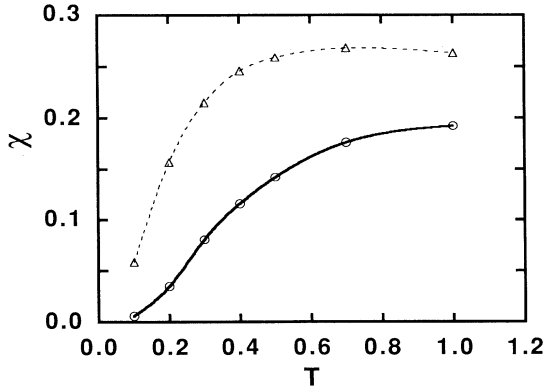

FIG. 4. Temperature dependence of the uniform spin susceptibility for $J=1.5$ (triangles) and $J=2.0$ (circles) in the case $\rho\sim0.6$ and $\gamma=t=1.0$.

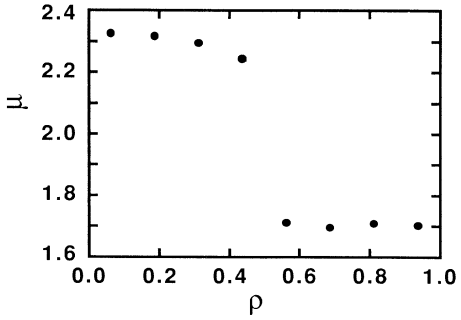

FIG. 5. Chemical potential μ vs filling factor ρ at $J=2.0$, $t=\gamma=1.0$.

confirmed in Fig. 3. In addition, the charge gap does not close at least until $J\sim1$ as seen in Fig. 3. It is not clear whether the charge gap remains for smaller J because of finite-size effects. Figure 5 illustrates the chemical potential vs filling at $J=2.0$, which shows the formation of a charge gap at quarter filling. The charge gap for the dimerized t-J model increases with the decrease of J similarly to the case of the charge gap of the attractive Hubbard model in the strong-coupling region. The charge gap Δ_c is estimated as $\Delta_c=0.63$, 0.53, and 0.26 at $J=1.5$, 2, and 4, respectively, for $t=\gamma=1.0$.

The critical exponent θ_c is obtained from the compressibility κ and the charge velocity v_c illustrated in Fig. 6 by using Eq. (3.5). The obtained result is shown in Fig. 7 for the case of $J=1.0$ and $t=\gamma=1.0$. Because of the tendency to charge-gap formation, θ_c has a dip at quarter filling $\rho=0.5$, where finite-size effect is large. Except this region, θ_c monotonically increases with the increase of the filling. Near half-filling, where the spin gap opens, the critical exponent θ_c also sharply increases indicating strong enhancement of the pairing correlation. As given in (1.5a) and (1.5b), the pairing correlation dominates over CDW correlation for $\theta_c>1$. The CDW correlation seems to be dominant only near quarter filling.

The pairing correlation of the type (1.2c) and (1.3a) is related to the order parameter of

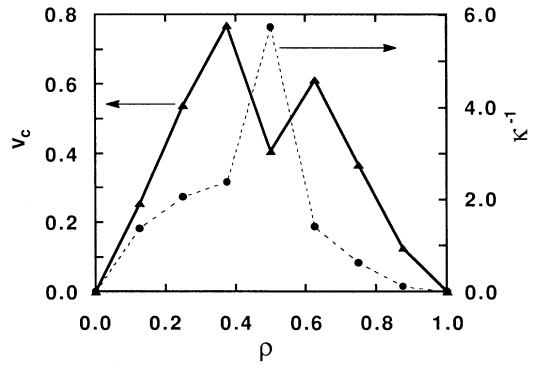

FIG. 6. Charge velocity v_c (triangles) and the inverse compressibility (circles) plotted as a function of the filling factor ρ.

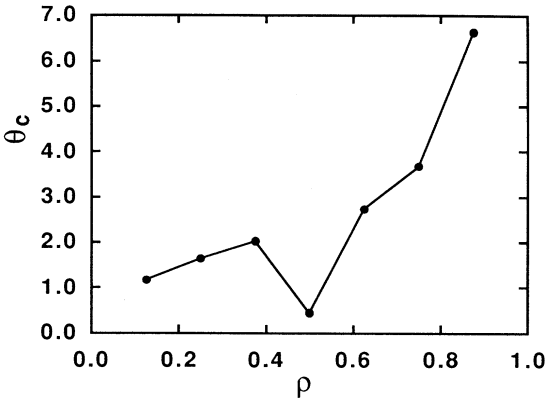

FIG. 7. The critical exponent θ_c as a function of the filling factor ρ.

$$O_S(q=0)=\frac{1}{\sqrt{2}}\sum_j (c_{j\uparrow}c_{j+1\downarrow}-c_{j\downarrow}c_{j+1\uparrow})$$
$$=\sqrt{2}\sum_k (\cos ka)c_{k\uparrow}c_{-k\downarrow} .$$

In the dimerized t-J model, the order parameter of the type

$$O_S(q=\pi)=\frac{1}{\sqrt{2}}\sum_j (-1)^j(c_{j\uparrow}c_{j+1\downarrow}-c_{j\downarrow}c_{j+1\uparrow})$$
$$=\sqrt{2}i\sum_k (\sin ka)c_{k\uparrow}c_{-k+\pi\downarrow}$$

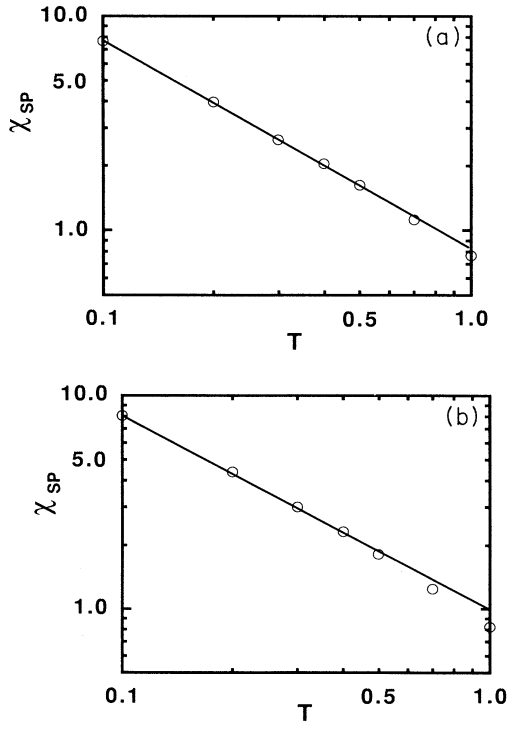

FIG. 8. Temperature dependence of the pairing susceptibility χ_{SP} for (a) $J=1.5$ and (b) $J=2.0$ at $t=\gamma=1.0$.

should also be taken into account as discussed.[11] The pairing correlation of

$$C_{SPQ}(r_i-r_j)=\langle O^{\dagger}_{SQi}O_{SQj}\rangle ,$$

with

$$O_{SQj}=\frac{(-1)^j}{\sqrt{2}}(c_{j\uparrow}c_{j+1\downarrow}-c_{j\downarrow}c_{j+1\uparrow})$$

shows the same power-law decay as $C_{SP}(r_i-r_j)$ and characterized by r^{-1/θ_c} as well.

At finite temperatures, the pairing susceptibility should show the behavior given in (1.6b) at sufficiently low temperatures. However, at moderately low temperatures, the pairing susceptibility obtained from the numerical transfer-matrix method shows somewhat weaker temperature dependence as is seen in Fig. 8, where the results are obtained from the Hamiltonian (2.2). The results from (2.1) are similar. Although it shows power-law divergence, the power seems to be smaller than that obtained from θ_c in Fig. 6. It indicates that the asymptotic behavior (1.6b) is restricted to very low-temperature region and a crossover should be seen below the temperatures shown in Fig. 8. In any case, the pairing correlation is the most dominant correlation for this model near half-filling at sufficiently low temperatures as well as at moderately low temperatures shown in Figs. 8.

IV. CONCLUSIONS AND DISCUSSIONS

We have investigated the phase diagram of the 1D dimerized t-J model by the exact-diagonalization method, the numerical transfer-matrix method and the quantum Monte Carlo method. The model has spin gap near half-filling and also in the strongly dimerized region. This spin-gap region is continuously connected with the strongly dimerized limit, where mapping of this model to the attractive Hubbard model is established. The gap region is also connected with the spin gap in the dimerized Heisenberg model as well as with the Haldane-gap state in the spin-1 Heisenberg model. In the spin-gap region, the correlation functions follow Luther-Emery fixed point at sufficiently low temperatures, where spin and charge are separated with the charge degrees of freedom showing Tomonaga-Luttinger liquid behavior. At finite temperatures, rich structure is expected with a crossover. The pairing correlation dominates over CDW correlation in the spin-gap region. The critical exponent shows that the divergence of the pairing susceptibility at low temperatures are stronger when one approaches closer to half-filling. At quarter filling, the charge gap opens at least for the dimerization larger than a threshold value, where the long-range order of CDW may exist. The attractive interaction is not introduced explicitly in the dimerized t-J model even in the spin-gap region, because the dimerized t-J modal can be derived as an effective Hamiltonian of a multiband Hubbard model with only repulsive interactions under dimerized lattice structure. If the quantum spin system with the dimerized exchange J is coupled to itinerant fermions with the transfer t by strong Kondo coupling J_K, the model is mapped to the dimerized t-J model. Although it introduces only repulsive in-

teraction in the original model, the effective Hamiltonian belongs to the same fixed point as the attractive Hubbard model. It is in marked contrast with the one-dimensional uniform t-J model where the spin gap does not appear at least near half-filling.[20]

Similar mechanisms for the pairing have also been discussed in different models. The 1D frustrated t-J model with the next-nearest-neighbor exchange coupling J' has been discussed by the author[9] as another example belonging to the Luther-Emery fixed point. In the limit $J \to 0$ with J'/J fixed large, the existence of the spin gap has been shown by Ogata, Luchini, and Rice near half-filling.[21] At finite J, it seems to be difficult at the moment to see the spin-gap region explicitly from finite cluster study because the spin gap seems to close very rapidly away from half-filling. Because the dimer order exists in the frustrated Heisenberg model,[22] the mechanism of the pairing should be essentially the same as that we have discussed in this paper if the spin gap persists away from half-filling. The 2D frustrated t-J model is another candidate of the spin gap in the region $J'/J \sim 0.5$, if the ground state has a dimer order. However, the nature of the ground state is not clear at this moment even for the half-filled case.

Recently, the double chain t-J model has been shown by Dagotto and co-workers[23,24] to have a spin gap even for intermediate strength of the interchain exchange coupling J'. The origin of the spin gap seems to be essentially the dimerization and the singlet formation of two fermions on different chains at the same site coupled by J'. This would provide another interesting example belonging to the Luther-Emery fixed point. The 2D analogy of this mechanism has been examined by Hida[25] in the half-filled system. It indicates that the spin-gap region is restricted to somewhat larger J'/J region (roughly $J'/J \geq 2.5$).

In the case of the dimerized t-J model, the spin gap may also exist in 2D for $\gamma \neq 0$. Generally speaking, the quasi-one-dimensional system is not favorable for the superconductivity as compared to the quasi-two-dimensional case because the localization effect is much more serious in realistic systems. In this respect, the 2D dimerized t-J model should be treated in the next step to clarify the mechanism of superconductivity along the line of this paper. The mean-field analysis of the pairing has been recently done in 2D dimerized t-J model providing a starting point for more reliable theoretical treatment.[11,26]

In one dimension, the ground state of the Heisenberg model shows an absence of the antiferromagnetic symmetry breaking. The spin degrees of freedom leaves a large amount of degeneracy in the ground state leading to a finite spin susceptibility, which is sometimes viewed from the formation of the spinon Fermi surface. The spin-gap formation resulted from the mean-field theory of spinon pairing in the uniform t-J model away from half-filling is an artifact of the mean-field treatment at least in one dimension. This fact seems to apply also to 2D Hubbard-type models. The condition for the spin-gap formation in 2D is a crucially important subject in clarifying the mechanism of high-temperature superconductivity and treatments beyond the mean-filed level are highly desired. The t-J model with nearest-neighbor Coulomb repulsion has recently been studied.[27,28] Small cluster study indicates the enhancement of pairing susceptibility near the phase separation boundary. It would be interesting further to explore the possibility of the spin-gap opening even near the phase separation boundary in the thermodynamic limit.

ACKNOWLEDGMENT

This work was financially supported by a Grant-in-Aid for Scientific Research on Priority Areas, Computational Physics as a New Frontier in Condensed Matter Research from the Ministry of Education, Science and Culture, Japan.

[1] J. Solyom, Adv. Phys. **28**, 209 (1979).
[2] V. J. Emery, *Highly Conducting One-Dimensional Solids,* edited by J. T. Devreese *et al.* (Plenum, New York, 1979), p. 327.
[3] A. Luther and V. J. Emery, Phys. Rev. Lett. **33**, 589 (1974).
[4] N. Kawakami and S.-K. Yang, Phys. Lett. A **148**, 359 (1990).
[5] H. Frahm and V. E. Korepin, Phys. Rev. B **42**, 10 553 (1990).
[6] N. Kawakakmi and S.-K. Yang. J. Phys. C **3**, 5983 (1991).
[7] T. Giamarchi and H. J. Schulz, Phys. Rev. B **39**, 4620 (1989).
[8] H. J. Schulz, in *Proceedings of Adriatico Research Conference and Workshop July 1990,* edited by G. Baskaran, A. E. Ruckenstein, E. Tosatti, and Yu Lu (World Scientific, Singapore, 1991), p. 57.
[9] M. Imada, J. Phys. Soc. Jpn. **60**, 1877 (1991).
[10] M. Imada, Physica C **185-189**, 1421 (1991).
[11] M. Imada, J. Phys. Soc. Jpn. **61**, 423 (1992).
[12] K. Okamoto, H. Nishimori, and Y. Taguchi, J. Phys. Soc. Jpn. **55**, 1458 (1986), and references therein.
[13] M. C. Cross and D. S. Fisher, Phys. Rev. B **19**, 402 (1979).
[14] S. Inagaki and H. Fukuyama, J. Phys. Soc. Jpn. **52**, 2504 (1983).
[15] K. Hida, Phys. Rev. B **45**, 2207 (1992).
[16] M. Imada, J. Phys. Soc. Jpn. **59**, 4121 (1990).
[17] M. Imada and Y. Hatsugai, J. Phys. Soc. Jpn. **58**, 3752 (1989).
[18] H. J. Schulz, Phys. Rev. Lett. **64**, 2831 (1990).
[19] F. D. M. Haldane, J. Phys. C **14**, 2585 (1981).
[20] The spin gap at low concentration near the phase separation has been claimed by M. Ogata, M. U. Luchini, S. Sorella, and F. F. Assaad, Phys. Rev. Lett. **66**, 2388 (1991).
[21] M. Ogata, M. U. Luchini, and T. M. Rice, Phys. Rev. B **44**, 12 083 (1991).
[22] T. Tonegawa and I. Harada, J. Phys. Soc. Jpn. **56**, 2153 (1987).
[23] E. Dagotto, in *Computational Approaches in Condensed Matter Physics,* Proceedings of the Nishinomiya-Yukawa Symposium, Nishinomiya, 1991, edited by S. Miyashita, M. Imada, and H. Takayama (Springer-Verlag, Berlin, 1992), p. 84.
[24] E. Dagotto, J. Riera, and D. J. Scalapino (unpublished).
[25] K. Hida, J. Phys. Soc. Jpn. **61**, 1013 (1992).
[26] M. Imada, Physica B (to be published).
[27] S. A. Kivelson, V. J. Emery, and H. Q. Lin, Phys. Rev. B **42**, 6523 (1990).
[28] E. Dagotto and J. Riera, Phys. Rev. B **46**, 12 084 (1992).